# Magnetic model refinement via a perturbation finite element method – from 1D to 3D

Patrick Dular
*ACE, Department of Electrical Engineering and Computer Science, University of Liège, Liège, Belgium and FNRS, Liège, Belgium*
Ruth V. Sabariego
*ACE, Department of Electrical Engineering and Computer Science, University of Liège, Liège, Belgium, and*
Laurent Krähenbühl
*Ampère (UMR CNRS 5005), École Centrale de Lyon, Université de Lyon, Écully, France*

## Abstract

**Purpose** The purpose of this paper is to develop a sub domain perturbation technique for refining magnetic circuit models with finite element (FE) models of different dimensions.

**Design/methodology/approach** A simplified problem considering ideal flux tubes is first solved, as either a 1D magnetic circuit or a simplified FE problem. Its solution is then corrected via FE perturbation problems considering the actual flux tube geometry and the exterior regions, that allow first 2D and then 3D leakage fluxes. Each of these sub problems requires an appropriate proper volume mesh, with no need of interconnection. The solutions are transferred from one problem to the other through projections of source fields between meshes.

**Findings** The developed perturbation FE method allows to split magnetic circuit analyses into subproblems of lower complexity with regard to meshing operations and computational aspects. A natural progression from simple to more elaborate models, from 1D to 3D geometries, is thus possible, while quantifying the gain given by each model refinement and justifying its utility.

**Originality/value** Approximate problems with ideal flux tubes are accurately corrected when accounting for leakage fluxes via surface sources of perturbations. The constraints involved in the subproblems are carefully defined in the resulting FE formulations, respecting their inherent strong and weak nature. As a result, an efficient and accurate computation of local fields and global quantities, i.e. flux, MMF, reluctance, is obtained. The method is naturally adapted to parameterized analyses on geometrical and material data.

**Keywords** Finite element analysis, Magnetic devices, Circuits

**Paper type** Research paper

## 1. Introduction

The perturbation of finite element (FE) solutions provides clear advantages in repetitive analyses (Badics *et al.*, 1997; Dular and Sabariego, 2007) and helps improving the solution accuracy (Dular *et al.*, 2007, 2008, 2009). It allows to benefit from previous

computations instead of starting a new complete FE solution for any variation of geometrical or physical data. It also allows different problem-adapted meshes and computational efficiency due to the reduced size of each subproblem.

A perturbation FE method is herein developed for refining the magnetic flux distribution in magnetic circuits starting from simplified models, based on ideal flux tubes defining 1D models, that evolve towards 2D and 3D accurate models. It is an extension of the method proposed in Dular *et al.* (2008, 2009), applied to refinements up to 3D models. From the so calculated field corrections, the associate corrections of global quantities proper to magnetic circuits, i.e. fluxes and magnetomotive forces (MMFs), are also evaluated to determine reluctances (Dular *et al.*, 2005). The method aims to build accurate reluctance networks, possibly starting from preliminary approximations (Chillet and Voyant, 2001). The developments are performed for the magnetic vector potential FE magnetostatic formulation, paying special attention to the proper discretization of the constraints involved in each subproblem. The method is illustrated and validated on test problems.

## 2. Magnetic model refinement

### *2.1 Series of coupled subproblems*

Instead of solving a complete problem with all its complexity and details, it is proposed to start from a simplified problem that is then refined. The initial assumptions are thus progressively canceled via successive model refinements, i.e. with well-posed subproblems.

Each subproblem is defined in its own domain, generally distinct from the complete domain. At the discrete level, this decreases the problem complexity and allows distinct meshes with suitable refinements. Many kinds of refinements can be considered (Dular *et al.*, 2007, 2008, 2009). Focus is here given to refinements from 1D to 3D models, leading to the coupling of 1D, 2D and 3D meshes.

A complete problem is thus split in a series of subproblems $p$ of an ordered set $P$. Its solution $\boldsymbol{u}$ is expressed as the sum of subproblem solutions $\mathbf{u}_p$, or corrections, i.e.:

$$\boldsymbol{u} \quad \sum\nolimits_{p\in P} \boldsymbol{u}_p. \tag{1}$$

In general, each subproblem $p$ is perturbed by all the other subproblems $q$ in $P$, i.e. all the subproblems are coupled. This is usually obvious for $p > q$ with the defined series. For $p < q$, it is the case when a correction becomes a significant source for any of its source problems, which is inherent to large perturbation problems. It is also the case in nonlinear analyses, thus even for $p \quad q$. These dependencies require iterations on the set $P$ to calculate each solution $\mathbf{u}_p$ as a series of corrections $\mathbf{u}_{p,i}$, i.e.:

$$\boldsymbol{u}_p \quad \sum\nolimits_i \boldsymbol{u}_{p,i} \quad \boldsymbol{u}_{p,1} + \boldsymbol{u}_{p,2} + \cdots, \tag{2}$$

where the calculation of $\mathbf{u}_{p,i}$ in a subproblem $p,i$ (problem $p$ with particular constraints at iteration $i$) is kept on till convergence up to a desired accuracy. Each correction must account for the influence of all the previous corrections $\mathbf{u}_{p,j}$ of the other subproblems, with $j$ the last iteration index for which a correction is known. Initial solutions $\mathbf{u}_{p,0}$ are set to zero. The global quantities linearly related to each correction, i.e. the fluxes and MMFs (Dular *et al.*, 2005), are added to obtain their complete values. This way, they gain in accuracy for the benefit of more accurate magnetic circuit models.

*2.2 Canonical magnetostatic problem*

A canonical magnetostatic problem $p$ is defined in a domain $\Omega_p$, with boundary $\partial\Omega_p \quad \Gamma_p \quad \Gamma_{h,p} \cup \Gamma_{b,p}$ (possibly at infinity). Subscript $p$ refers to the associated problem $p$. The equations, material relations, boundary conditions (BCs) and interface conditions (ICs) of problem $p$ are:

$$\text{curl } \boldsymbol{h}_p \quad \boldsymbol{j}_p, \quad \text{div } \boldsymbol{b}_p \quad 0, \tag{3a-b}$$

$$\boldsymbol{b}_p \quad \mu_p \boldsymbol{h}_p + \boldsymbol{b}_{s,p}, \quad \boldsymbol{j}_p \quad \boldsymbol{j}_{s,p}, \tag{3c-d}$$

$$\boldsymbol{n} \times \boldsymbol{h}_p|_{\Gamma_{h,p}} \quad 0, \quad \boldsymbol{n} \cdot \boldsymbol{b}_p|_{\Gamma_{b,p}} \quad 0, \tag{3e-f}$$

$$[\boldsymbol{n} \times \boldsymbol{h}_p]_{\gamma_p} \quad \boldsymbol{j}_{su,p}, \quad [\boldsymbol{n} \cdot \boldsymbol{b}_p]_{\gamma_p} \quad \boldsymbol{b}_{su,p}, \tag{3g-h}$$

where $\boldsymbol{h}_p$ is the magnetic field, $\boldsymbol{b}_p$ is the magnetic flux density, $\boldsymbol{j}_p$ is the electric current density, $\mu_p$ is the magnetic permeability and $\boldsymbol{n}$ is the unit normal exterior to $\Omega_p$.

The fields $\boldsymbol{b}_{s,p}$ and $\boldsymbol{j}_{s,p}$ are volume sources. The source $\boldsymbol{b}_{s,p}$ is usually used for fixing a remnant induction in magnetic materials. The source $\boldsymbol{j}_{s,p}$ fixes the current density in inductors. With the perturbation method, $\boldsymbol{b}_{s,p}$ is also used for expressing changes of permeability and $\boldsymbol{j}_{s,p}$ for adding portions of inductors (Dular *et al.*, 2008). In magnetodynamic problems, $\boldsymbol{j}_{s,p}$ also expresses changes of conductivity (Dular and Sabariego, 2007). Analogously to relation (3c), one can have $\boldsymbol{h}_p \quad \mu_p^{\ 1} \ \boldsymbol{b}_p + \boldsymbol{h}_{s,p}$ with the volume source $\mathbf{h}_{s,p}$.

The notation $[\cdot]_\gamma \quad \cdot|_\gamma + \quad \cdot|_{\gamma^-}$ expresses the discontinuity of a quantity through any interface $\gamma$ (with sides $\gamma^+$ and $\gamma$ ) in $\Omega_p$ (the region in between is considered to be exterior to $\Omega_p$). The associated surface fields $\boldsymbol{j}_{su,p}$ and $\boldsymbol{b}_{su,p}$ are generally zero, defining classical ICs for the physical fields, i.e. the continuities of the tangential component of $\boldsymbol{h}_p$ and of the normal component of $\boldsymbol{b}_p$. If nonzero, they define possible surface sources that account for particular phenomena occurring in the idealized thin region between $\gamma^+$ and $\gamma$ .

For the refinement of flux tubes, each problem $p$ is to be constrained via the so defined surface sources from parts of the solution of other problems. This is a key element of the developed method, that can be generalized to both 2D and 3D problems.

## 3. Refinement of flux tubes

*3.1 Parallel perturbations: considering leakage flux*

In a first problem, e.g. $p \quad 1$, the magnetic flux is forced to flow only in a subregion with perfect flux walls, i.e. a set of flux tubes $\Omega_1 \quad \Omega_{ft,1}$ of the complete domain $\Omega$. A second problem, e.g. $p \quad 2$, considers then that some flux wall portions become permeable. This allows leakage flux in the exterior region $\Omega \backslash \Omega_1$ and leads to a change of the flux distribution in $\Omega_1$. This procedure defines a so-called parallel perturbation, offering other parallel paths to the flux. A solution refinement is thus achieved.

There is a certain freedom to choose the flux wall portions to be perturbed and the sequence of such perturbations (Figure 1). Leakage flux can be first allowed in a 2D model (Dular *et al.*, 2008, 2009) before being extended in the third direction, i.e. in 3D. Once flux walls become progressively permeable, the actual geometry of the inductors can be taken into account.

In problem 1, the ideal flux tubes are considered with a zero normal magnetic flux density BC on their boundaries or flux walls $\Gamma_{ft,1} \quad \partial\Omega_1$. The trace of the magnetic field is unknown on $\Gamma_{ft,1}$. Once determined from the solution in $\Omega_1$, it can be used as a

BC to calculate the solution in $\Omega\backslash\Omega_1$, with all the precise characteristics of this exterior region (e.g. inductors and other surrounding regions). This task is however avoided, preferring the magnetic field to be simply zero in $\Omega\backslash\Omega_1$. With that purpose, problem 1 gathers all the inductor parts of the exterior region inside the double layer defined by $\Gamma^+_{ft,1}$ and $\Gamma_{ft,1}$, the inner and outer sides of $\Gamma_{ft,1}$ with regard to $\Omega_1$ (Figure 2, left). This defines idealized inductors and allows the magnetic field to be zero in $\Omega\backslash\Omega_1$. Each problem $p > 1$ must then correct the already obtained solutions, in particular solution 1, via particular corrections of ICs (Figure 2, right). Such ICs are surface sources (or interface-type sources) fixing the possible trace discontinuities of $\boldsymbol{h}_p$ and $\boldsymbol{b}_p$ in terms of other solutions $q$. The forced discontinuities introduced in a problem are thus to be corrected by another one.

The BCs of problem 1 are thus:

$$\boldsymbol{n}\cdot\boldsymbol{b}_1|_{\Gamma^+_{ft,1}} \quad 0, \quad \boldsymbol{n}\cdot\boldsymbol{b}_1|_{\Gamma^-_{ft,1}} \quad 0, \tag{4a-b}$$

$$\boldsymbol{n}\times\boldsymbol{h}_1|_{\Gamma^+_{ft,1}} \quad \boldsymbol{j}_{su,1}, \quad \boldsymbol{n}\times\boldsymbol{h}_1|_{\Gamma^-_{ft,1}} \quad 0, \tag{5a-b}$$

which establishes the discontinuities or ICs:

$$[\boldsymbol{n}\cdot\boldsymbol{b}_1]_{\Gamma_{ft,1}} \quad \boldsymbol{b}_{su,1} \quad 0, \quad [\boldsymbol{n}\times\boldsymbol{h}_1]_{\Gamma_{ft,1}} \quad \boldsymbol{j}_{su,1}. \tag{6a-b}$$

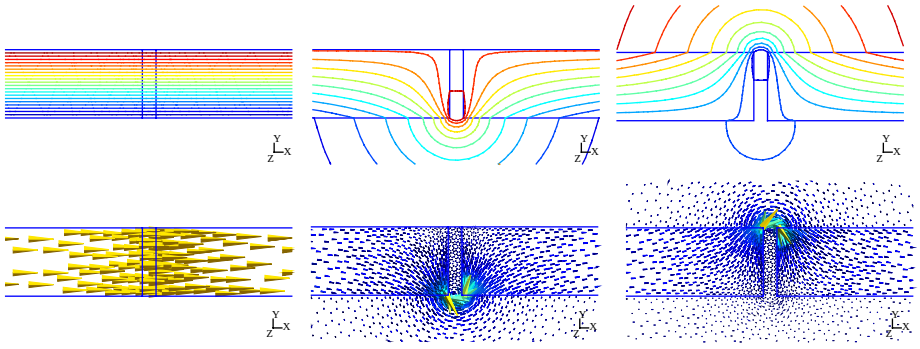

**Figure 1.**
Field lines (top) and magnetic flux density (bottom) of the initial problem with an ideal flux tube ($\boldsymbol{b}_1$, left), its local correction below ($\boldsymbol{b}_2$, middle) and above the air gap ($\boldsymbol{b}_3$, right)

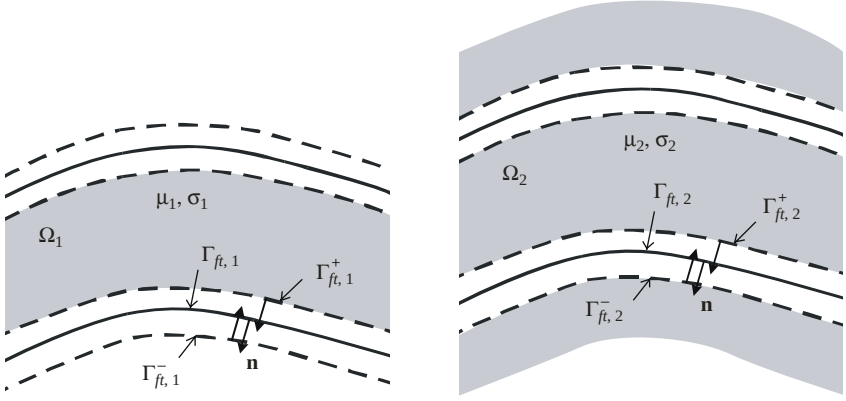


**Figure 2.**
Domains for the ideal (left) and real (right) flux tube problems

Problem 2 must correct the solution 1 via appropriate ICs (3g-h). On the one hand, one has:

$$[\boldsymbol{n}\cdot\boldsymbol{b}_2]_{\Gamma_{ft,2}} \quad \boldsymbol{b}_{su,2} \quad [\boldsymbol{n}\cdot\boldsymbol{b}]_{\Gamma_{ft,2}} \quad \boldsymbol{b}_{su,1} \quad 0, \tag{7}$$

due to the known continuity of $\boldsymbol{n}\cdot\boldsymbol{b}$ in the complete solution (1) and the zero value of $\boldsymbol{b}_{su,1}$ via equation (6a). On the other hand, one has:

$$[\boldsymbol{n}\times\boldsymbol{h}_2]_{\Gamma_{ft,2}} \quad \boldsymbol{j}_{su,2} \quad [\boldsymbol{n}\times\boldsymbol{h}]_{\Gamma_{ft,2}} \quad \boldsymbol{j}_{su,1} \quad \boldsymbol{n}\times\boldsymbol{h}_1|_{\Gamma^+_{ft,1}}, \tag{8}$$

due to the known continuity of $\boldsymbol{n}\times\boldsymbol{h}$ in the complete solution (1) and relation (5a). Problem 2 extends then the solution out of the flux tubes and corrects it in the tubes. IC (8) can be seen as a surface source acting on both sides of $\Gamma_{ft,2}$. Note that $\Gamma_{ft,2}$ is similar to $\Gamma_{ft,1}$. They only differ at the discrete level due to their different supporting meshes.

### *3.2 Series perturbations: connecting two flux tubes*

Prior to considering leakage flux, the series connection of two ideal flux tubes can be refined using the same kind of surface sources as in the parallel perturbations, this time as a so-called series perturbation. The field distribution in each tube can be first easily constructed via geometrical considerations, i.e. no need of FE analysis (Figure 3, left). In general, the flux conservation from one tube to the other can be expressed exactly. Consequently, the junction surface now acts as an interface $\Gamma_{ft,1}$, through which the continuity of the normal magnetic flux density is satisfied ($[\boldsymbol{n}\cdot\boldsymbol{h}_1]_{\Gamma_{ft,1}}$ 0) and the discontinuity of the tangential magnetic field is simply quantifiable ($[\boldsymbol{n}\times\boldsymbol{b}_1]_{\Gamma_{ft,1}} \neq 0$). The correction problem ($p$ 2) to be solved is thus defined with the following ICs:

$$[\boldsymbol{n}\cdot\boldsymbol{b}_2]_{\Gamma_{ft,2}} \quad [\boldsymbol{n}\cdot\boldsymbol{b}_1]_{\Gamma_{ft,1}} \quad 0, \tag{9}$$

$$[\boldsymbol{n}\times\boldsymbol{h}_2]_{\Gamma_{ft,2}} \quad [\boldsymbol{n}\times\boldsymbol{b}_1]_{\Gamma_{ft,1}}. \tag{10}$$

It can be limited to a certain neighborhood $\Omega_2$ on both sides of the interface $\Gamma_{ft,2}$ $\Gamma_{ft,1}$ (Figure 3, middle).

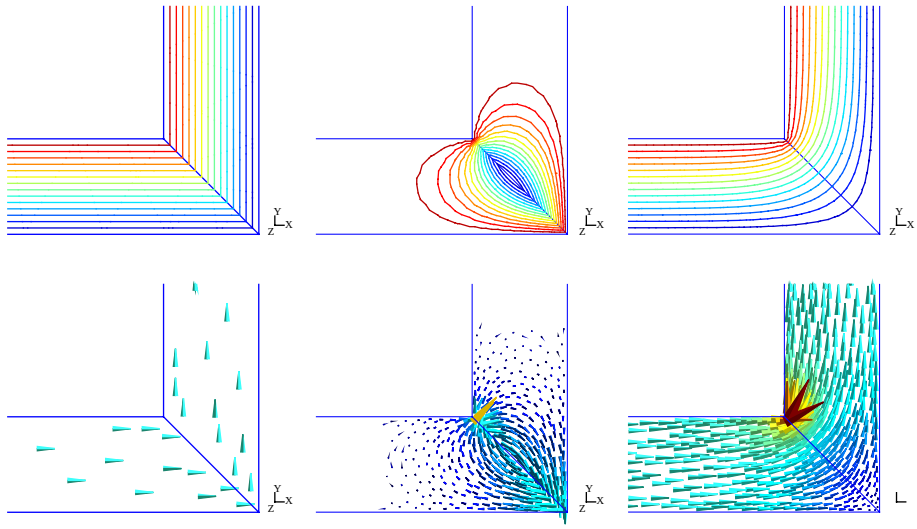

**Figure 3.**
Field lines (top) and magnetic flux density (bottom) of the initial problem with two ideal flux tubes in series ($\boldsymbol{b}_1$, left), its local correction at the junction ($\boldsymbol{b}_2$, middle) and the complete solution ($\boldsymbol{b}$, right)

## 4. Finite element weak formulations

### *4.1 b-Conform weak formulations*

The canonical problem $p$ (equations (3a-h)) is defined in $\Omega_p$ with the magnetic vector potential formulation (Dular *et al.*, 2005), expressing the magnetic flux density $\boldsymbol{b}_p$ in $\Omega_p$ as the curl of a magnetic vector potential $\boldsymbol{a}_p$. The related $\boldsymbol{a}$-formulation is obtained from the weak form of the Ampère equation (3a) (Dular *et al.*, 2005):

$$\begin{aligned}(\mu_p\,{}^{1}\mathrm{curl}\boldsymbol{a}_p,\ \mathrm{curl}\boldsymbol{a}')_{\Omega_p} \quad (\boldsymbol{h}_{s,p},\ \mathrm{curl}\boldsymbol{a}')_{\Omega_p} \quad (\boldsymbol{j}_{s,p},\ \boldsymbol{a}')_{\Omega_p} + \langle \boldsymbol{n}\times\boldsymbol{h}_{s,p},\ \boldsymbol{a}'\rangle_{\Gamma_{h,p}} \\ + \langle \boldsymbol{n}\times\boldsymbol{h}_p, \boldsymbol{a}'\rangle_{\Gamma_{b,p}} + \langle [\boldsymbol{n}\times\boldsymbol{h}_p]_{\gamma_p},\ \boldsymbol{a}'\rangle_{\gamma_p} \quad 0, \quad \forall\, \boldsymbol{a}' \in F^1_p(\Omega_p),\end{aligned} \tag{11}$$

where $F^1_p(\Omega_p)$ is a gauged curl-conform function space defined on $\Omega_p$ and containing the basis functions for $\boldsymbol{a}$ as well as for the test function $\boldsymbol{a}'$ (at the discrete level, this space is defined by edge FEs); $(\cdot,\cdot)_\Omega$ and $<\cdot,\cdot>_\Gamma$, respectively, denote a volume integral in $\Omega$ and a surface integral on $\Gamma$ of the product of their vector field arguments. With the $\boldsymbol{b}$-conform formulation used, ICs (3h) and (3g) are to be defined, respectively, in strong and weak senses (essential and natural ICs), i.e. in $F^1_p(\Omega_p)$ and in a surface integral term. The surface integral term on $\Gamma_{h,\mathrm{p}}$ accounts for natural BCs of type (3e), usually with $\boldsymbol{n}\times\boldsymbol{h}_{s,p}|_{\Gamma_{h,p}}$ 0. The unknown term on the surface $\Gamma_{b,p}$ with essential BCs on $\boldsymbol{n}\cdot\boldsymbol{b}_p$ is usually omitted because it does not locally contribute to equation (11). It will be shown to be the key for the post-processing of a solution $p$, a part of which, $\boldsymbol{n}\times\boldsymbol{h}_p|_{\Gamma_{b,p}}$, is used as a source in further problems.

### *4.2 Surface sources for leakage flux*

For the ideal flux tubes $\Omega_{ft,1}$ of problem $p$ 1, BC (4a) leads to an essential BC on the primary unknown $\boldsymbol{a}_1$ that can be expressed in general (in 3D) via the definition of a surface scalar potential $u_1$ (Dular *et al.*, 2005), i.e.:

$$\boldsymbol{n}\cdot\mathrm{curl}\boldsymbol{a}_1|_{\Gamma_{ft,1}} \quad 0 \Leftrightarrow \boldsymbol{n}\times\boldsymbol{a}_1|_{\Gamma_{ft,1}} \quad \boldsymbol{n}\times\mathrm{grad}u_1|_{\Gamma_{ft,1}}. \tag{12}$$

This potential is multi-valued because a net magnetic flux flows in $\Omega_{ft,1}$. Its discontinuity through cut lines, making the boundary $\Gamma_{ft,1}$ simply connected, is directly related to the net flux. In 2D, the flux wall BC amounts to define a floating magnetic vector potential $\boldsymbol{a}_1$ (with a constant perpendicular component) on each non-connected part of $\Gamma_{ft,1}$.

Formulation $p$ 1 is obtained from equation (11) with $\boldsymbol{h}_{s,1}$ 0, $\boldsymbol{j}_{s,1}$ 0, $\boldsymbol{n}\times\boldsymbol{b}_{s,1}|_{\Gamma_{h,1}}$ 0, $\Gamma_{ft,1}\subset\Gamma_{b,1}$ and $\gamma_1$ $\varnothing$. The surface integral term $<\boldsymbol{n}\times\boldsymbol{h}_1,\ a'>_{\Gamma_{ft,1}}$ differs from zero only for the test function $a'$ grad $u'$ (from equation (12)), the value of which is then the MMF $F_1$ associated with a flux tube (this can be demonstrated from the general procedure developed in Dular *et al.*, 2005). It is zero for all the other local test functions (at the discrete level, for any edge not belonging to $\Gamma_{ft,1}$). This way, the magnetic circuit relation can be expressed for each flux tube $\Omega_{ft,1}$, to relate fluxes and MMFs.

The correction formulation $p$ 2 is then obtained from equation (11) with $\boldsymbol{h}_{s,2}$ 0, $\boldsymbol{n}\times\boldsymbol{b}_{s,2}|_{\Gamma_{h,2}}$ 0 and $\gamma_2$ $\Gamma_{ft,2}$. The volume source current density $\boldsymbol{j}_{s,2}$ is now defined in the inductor portions added to the studied domain $\Omega_2$, in place of the first idealized inductors. IC (7) is strongly expressed via the essential tangential continuity of the vector potential $\boldsymbol{a}_2$ through $\Gamma_{ft,2}$. IC (8) can rather only act in a weak sense via the surface integral term related to $\gamma_2$ $\Gamma_{ft,2}$ in equation (11).

Indeed, the involved surface source $\boldsymbol{n} \times \boldsymbol{h}_1$ is not known in a strong sense on $\Gamma_{ft,2}$, but rather in a weak sense. One has, with equations (8) and (11) for $p$ 1:

$$\langle [\boldsymbol{n} \times \boldsymbol{h}_2]_{\Gamma_{ft,2}}, \ \boldsymbol{a}' \rangle_{\Gamma_{ft,2}} \quad \langle \quad \boldsymbol{n} \times \boldsymbol{h}_1, \ \boldsymbol{a}' \rangle_{\Gamma^+_{ft,2}} \quad \langle \quad \boldsymbol{n} \times \boldsymbol{h}_1, \ \boldsymbol{a}' \rangle_{\Gamma^+_{ft,1}}$$

$$(\mu_1^{\ 1} \ \mathrm{curl}\boldsymbol{a}_1, \ \mathrm{curl}\boldsymbol{a}')_{\Omega_{ft,1}=\Omega_{ft,2}}. \tag{13}$$

This way, the surface integral source term on $\gamma_2$ $\Gamma_{ft,2}$ in equation (11) is calculated from a volume integral coming from the previous problem 1. Its consideration via a volume integral, limited at the discrete level to one single layer of FEs touching the boundary, is the natural way to average it as a weak quantity. Any other kind of evaluation would not be consistent with the FE formulation used.

At the discrete level, the source quantity $\boldsymbol{a}_1$ in equation (13), initially given in mesh 1, has to be projected in mesh 2 in a domain $\Omega_{s,2}$ limited to the layer of FEs touching $\Gamma_{ft,2}$. This can be done via a Galerkin projection method (Geuzaine *et al.*, 1999) of its curl limited to $\Omega_{s,2}$, i.e.:

$$(\mathrm{curl}\boldsymbol{a}_{1,2\ proj}, \ \mathrm{curl}\boldsymbol{a}')_{\Omega_{s,2}} \quad (\mathrm{curl}\boldsymbol{a}_1, \ \mathrm{curl}\boldsymbol{a}')_{\Omega_{s,2}}, \quad \forall \ \boldsymbol{a}' \in F^1_2(\Omega_{s,2}), \tag{14}$$

where $F^1_2(\Omega_{s,2})$ is a gauged curl-conform function space for the 2-projected source $\boldsymbol{a}_{1,2\text{-}proj}$ (the projection of $\boldsymbol{a}_1$ on mesh 2) and the test function $\boldsymbol{a}'$. Directly projecting $\boldsymbol{a}_1$ (not its curl) would result in numerical inaccuracies when evaluating its curl.

The test function $\boldsymbol{a}'$ in equation (13) is associated only with the edges of $\Gamma_{ft,2}$; the support of the function curl $\boldsymbol{a}'$ is indeed limited to this layer. This reduced support decreases the computational effort of the projection process.

*4.3 Surface sources for a series connection of flux tubes*

The local FE problem to be solved in the neighborhood of a junction interface $\Gamma_{ft,2}$ $\Gamma_{ft,1}$ of two flux tubes is still expressed by equation (11). IC (9) leads to the tangential continuity of the vector potential $\boldsymbol{a}_2$ through $\Gamma_{ft,2}$. IC (10) is weakly expressed via the surface source integral term:

$$\langle [\boldsymbol{n} \times \boldsymbol{h}_2]_{\Gamma_{ft,2}}, \ \boldsymbol{a}' \rangle_{\Gamma_{ft,2}} \quad \langle \quad [\boldsymbol{n} \times \boldsymbol{h}_1]_{\Gamma_{ft,1}}, \ \boldsymbol{a}' \rangle_{\Gamma_{ft,2}}, \tag{15}$$

which is simply calculated from the known distribution of $\boldsymbol{h}_1$ on both sides of $\Gamma_{ft,1}$.

## 5. Application

Two problems are considered to test and illustrate the refinement method from 1D to 3D models.

A stranded inductor is first studied (Figure 4). Its cross section in the XY plane initially defines an initial 2D model, with the solution shown in Figure 4 (left). This 2D solution is considered to be invariant in the Z direction up to a certain distance (z 100 mm). Beyond this distance, the field is chosen to be zero, which results in a particular IC to be further corrected. This solution then serves as an IC constraint (8) for a 3D perturbation model considering the inductor end winding.

A part of the correction is shown in a plane crossing the end winding, where its significance in the direct vicinity of this end region is pointed out (Figure 4, right).

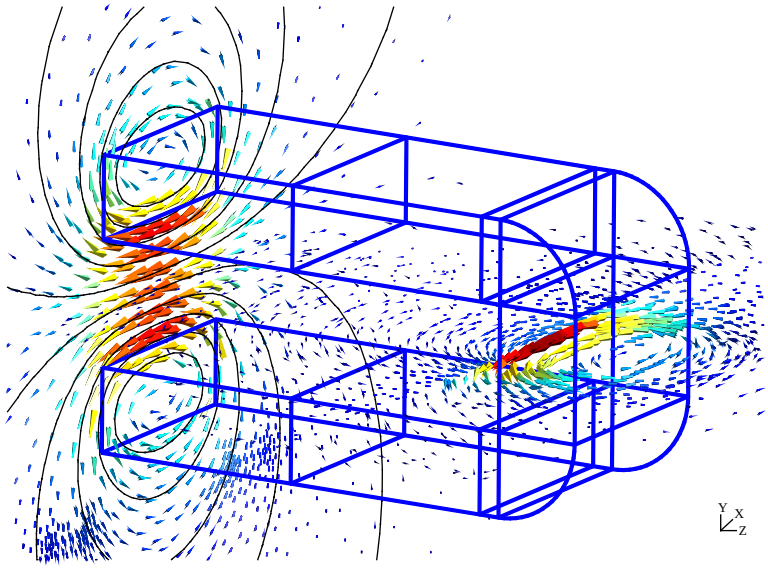


**Notes:** Solution of the 2D model in the XY plane (z = 0) (vector field and field lines, left) and a part of the 3D correction in a particular plane crossing the end winding (right)

**Figure 4.**
Magnetic flux density generated by a stranded inductor (half geometry)

Another part is shown along a line centered with the inductor and following its main (Z) direction (Figure 5).

The current density distribution considered for the 2D model is implicitly the one shown in Figure 6, left. Once this distribution has been used in 2D, the 3D perturbation model only needs its complementary part defined in the end windings (Figure 6, right).

An electromagnet is then studied (Figure 7). It consists of a U-shape core surrounded by a stranded inductor and separated from an I-shape core via two air gaps. For both core, the width and depth are 20 and 100 mm, respectively. Their relative

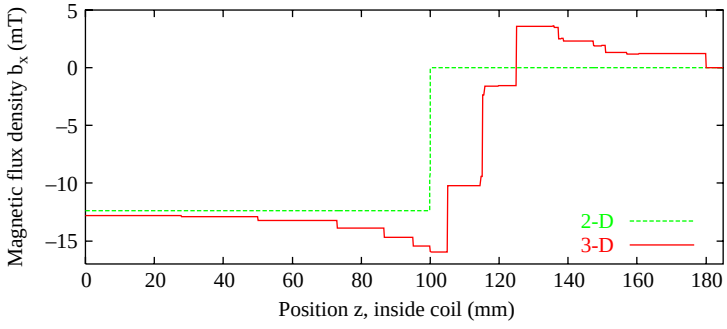


**Notes:** Solution of the 2D model (implicitly extended as a constant up to z = 100 mm) and 3D solution after correction in the vicinity of the end winding

**Figure 5.**
Magnetic flux density along the main (Z) direction of the inductor (from its center)

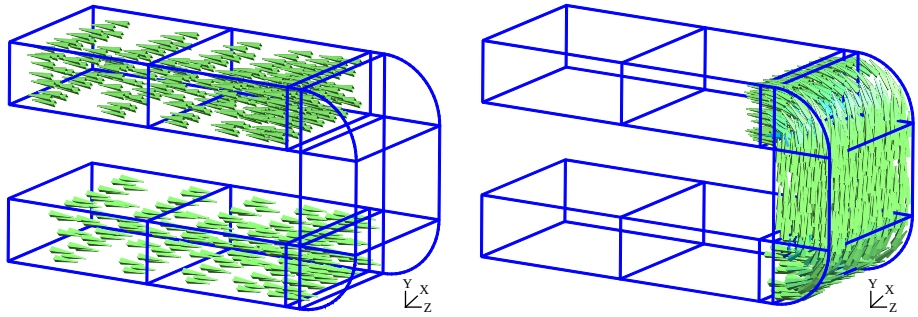


**Figure 6.**
Source current density in the inductor

**Notes:** Its implicit distribution for the 2D model (left) and its complementary part in the end winding for the 3D perturbation model (right)

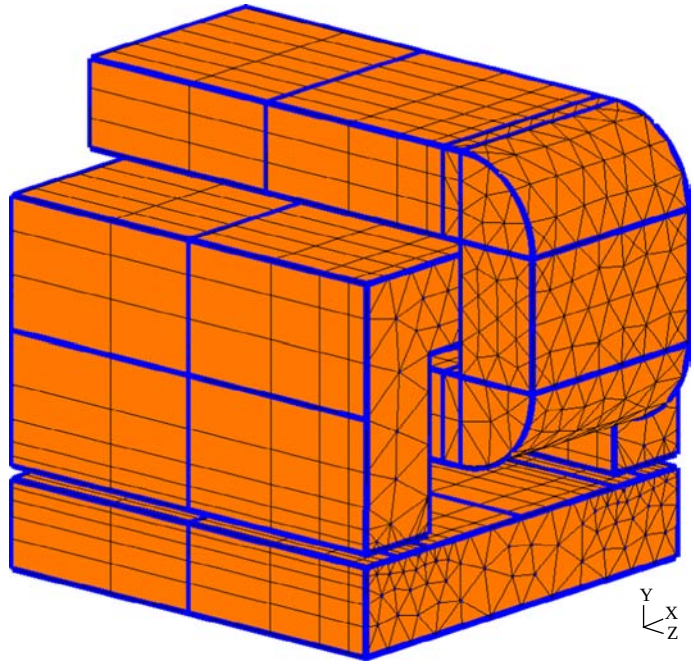


**Figure 7.**
3D model of the electromagnet

permeability is $\mu_{r,U\ core}$ $\mu_{r,I\ core}$ 500. Each gap is 3 mm. Other values of the permeability and the air gap will be considered as well for parameterized analyses.

A 2D solution is first calculated (Figure 8). It can be either obtained directly or from a sequence of correction problems starting from a 1D model progressively refined in 2D with consideration of 2D leakage fluxes (Dular *et al.*, 2008, 2009). This solution serves then as a source for a perturbation problem allowing leakage flux in 3D, in the same way it has been done with only the inductor. Significant corrections near the end winding and the air gaps are shown (Figures 9 and 10). The 3D problem calculates the actual flux

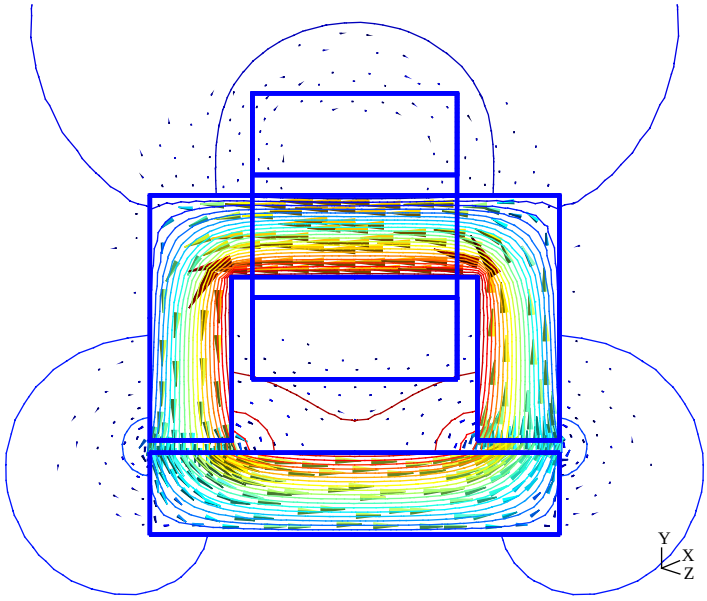


**Note:** Magnetic flux density and field lines

**Figure 8.**
2D cross section of the electromagnet and solution

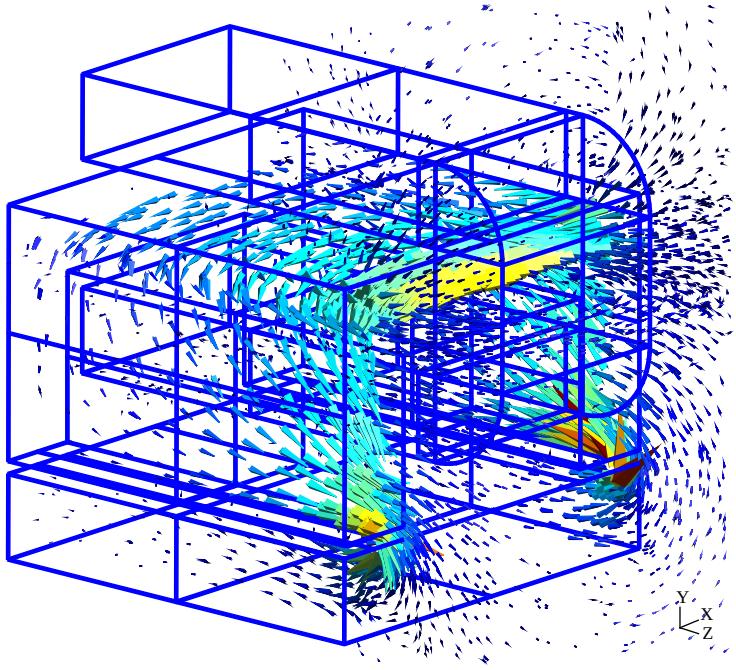


**Note:** Solution of the 3D correction in particular planes near the end winding and the air gaps

**Figure 9.**
Magnetic flux density

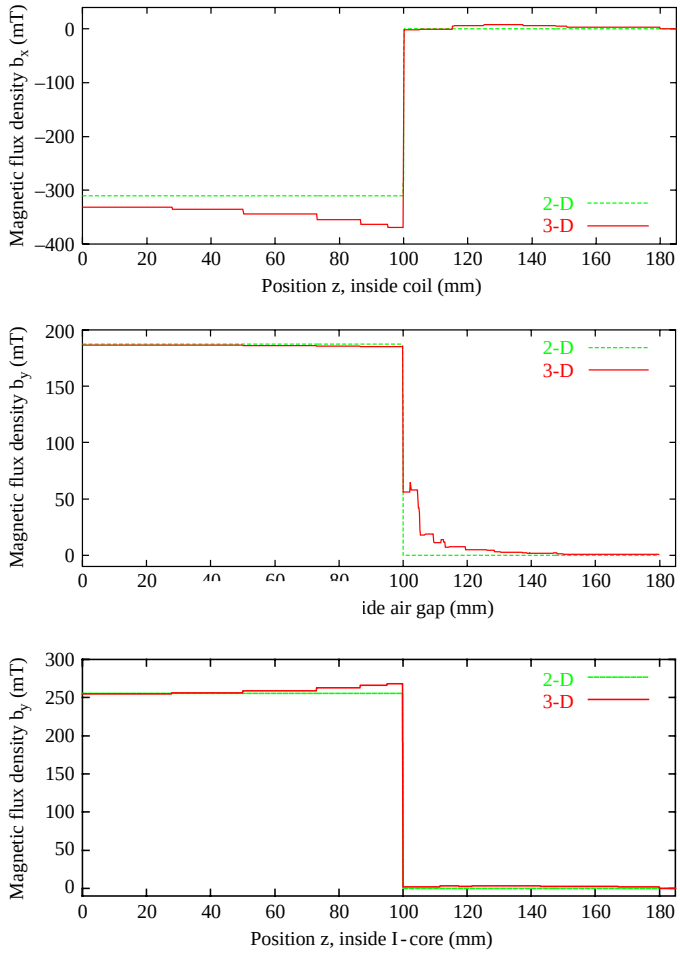


**Figure 10.**
Magnetic flux density along Z direction in the 3D system

**Notes:** Solution of the 2D model (implicitly extended as a constant up to z = 100 mm) and 3D solution after corrections in the vicinity of the end winding (top), the air gap (middle) and the I-core (bottom)

distribution in the vicinity of the inductor end winding and in the vicinity of the cores, with its own adapted mesh. It also corrects the flux density in the cores and the air gaps.

Each correction properly modifies the inductor flux linkage. This is shown for air gaps of 1 and 3 mm in Figures 11 and 12, respectively. The 1D model simply considers ideal flux tubes of constant sections. It is then followed by a 2D model considering ideal flux tubes with their actual geometry (corners are thus accurately taken into account). Then leakage fluxes in and out of the flux tubes are considered in 2D as well, before extension in the third dimension (3D). In general, each additional leakage flux correction significantly influences the inductor flux linkage. The 3D correction is lower for low reluctances of the magnetic circuit (i.e. for high permeability and small air gap).

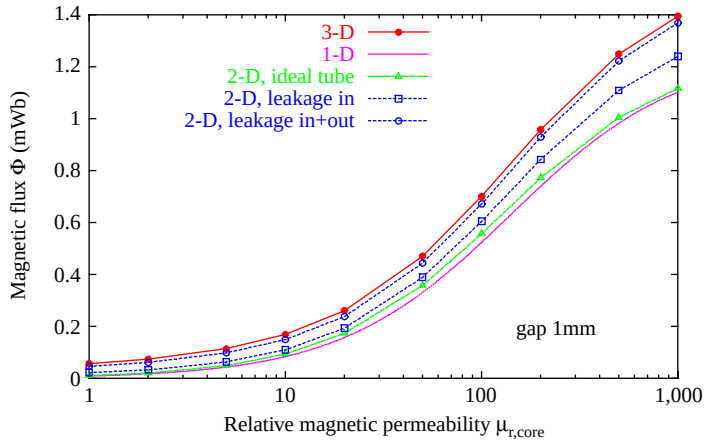


**Figure 11.**
Inductor flux linkage versus the core magnetic permeability (air gap thickness of 1 mm) updated after each model refinement

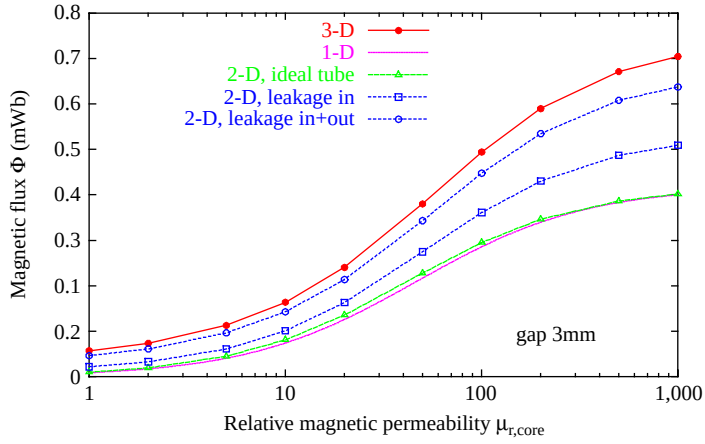


**Figure 12.**
Inductor flux linkage versus the core magnetic permeability (air gap thickness of 3 mm) updated after each model refinement

The relative corrections obtained for model refinements from 1D to 2D and from 2D to 3D are given in Figures 13 and 14, respectively, for different air gaps (0, 1 and 3 mm) in function of the permeability of the magnetic cores. Neglecting 2D leakage fluxes obviously amounts to large errors (about 50 per cent) in magnetic circuits with higher reluctances (e.g. larger air gaps and/or lower permeability). Neglecting 3D leakage fluxes amounts to an error up to 25 per cent for the considered geometry. The error will be higher with flatter magnetic circuits.

For each series of subproblems, the convergence of the solution depends on the extension of the subdomains. The more extended the subdomains are, the faster the convergence is. At the limit, if the successive subdomains progressively cover the complete domain, no iterations are needed. This paper focuses on the practical aspects of the method, mainly the surface sources that can appear in perturbation FE analyses from 1D to 3D. The study of the convergence, with the choice of the subdomains, is to be done further as an extension of this preliminary paper.

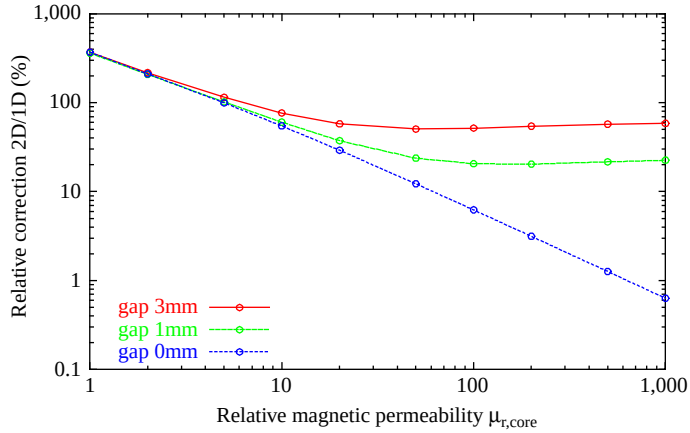


**Figure 13.**
Relative correction from 1D to 2D models versus the core magnetic permeability for different air gap thicknesses

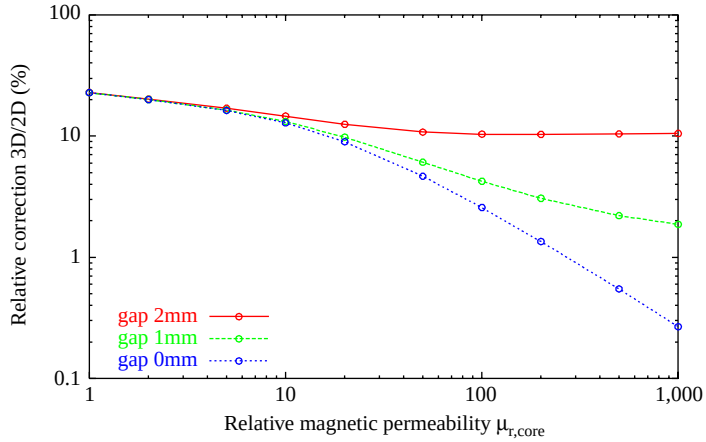


**Figure 14.**
Relative correction from 2D to 3D models versus the core magnetic permeability for different air gap thicknesses

## 6. Conclusions

The developed perturbation FE method allows to split magnetic circuit analyses into subproblems of lower complexity with regard to meshing operations and computational aspects. A natural progression from simple to more elaborate models, from 1D to 3D geometries, is thus possible, while quantifying the gain given by each model refinement and justifying its utility. Approximate problems with ideal flux tubes are accurately corrected when accounting for leakage fluxes via surface sources of perturbations. The constraints involved in the subproblems have been carefully defined in the resulting FE formulations, respecting their inherent strong and weak nature. As a result, an efficient and accurate computation of local fields and global quantities, i.e. flux, MMF, reluctance, is obtained. The method is naturally adapted to parameterized analyses on geometrical and material data.

Further work is in progress for defining additional types of subproblems, e.g. to apply successive perturbations accounting for nonlinear and eddy current models. An adaptation of the domain of each subproblem has to be also studied, together with its effect on the convergence of the complete solution.

## References

Badics, Z., Matsumoto, Y., Aoki, K., Nakayasu, F., Uesaka, M. and Miya, K. (1997), "An effective 3 D finite element scheme for computing electromagnetic field distorsions due to defects in eddy current nondestructive evaluation", *IEEE Transactions on Magnetics*, Vol. 33 No. 2, pp. 1012 20.

Chillet, C. and Voyant, J.Y. (2001), "Design oriented analytical study of a linear electromagnetic actuator by means of a reluctance network", *IEEE Transactions on Magnetics*, Vol. 37 No. 4, pp. 3004 11.

Dular, P. and Sabariego, R.V. (2007), "A perturbation method for computing field distortions due to conductive regions with h conform magnetodynamic finite element formulations", *IEEE Transactions on Magnetics*, Vol. 43 No. 4, pp. 1293 6.

Dular, P., Gyselinck, J., Henneron, T. and Piriou, F. (2005), "Dual finite element formulations for lumped reluctances coupling", *IEEE Transactions on Magnetics*, Vol. 41 No. 5, pp. 1396 9.

Dular, P., Sabariego, R.V., Gyselinck, J. and Krahenbuhl, L. (2007), "Sub domain finite element method for efficiently considering strong skin and proximity effects", *COMPEL: The International Journal for Computation and Mathematics in Electrical and Electronic Engineering*, Vol. 26 No. 4, pp. 974 85.

Dular, P., Sabariego, R.V., Ferreira da Luz, M.V., Kuo Peng, P. and Krahenbuhl, L. (2008), "Perturbation finite element method for magnetic circuits", *IET Science, Measurement & Technology*, Vol. 2 No. 6, pp. 402 8.

Dular, P., Sabariego, R.V., Ferreira da Luz, M.V., Kuo Peng, P. and Krahenbuhl, L. (2009), "Perturbation finite element method for magnetic model refinement of air gaps and leakage fluxes", *IEEE Transactions on Magnetics*, Vol. 45 No. 3 (in press).

Geuzaine, C., Meys, B., Henrotte, F., Dular, P. and Legros, W. (1999), "A Galerkin projection method for mixed finite elements", *IEEE Transactions on Magnetics*, Vol. 35 No. 3, pp. 1438 41.

## About the authors

Patrick Dular received the Electrical Engineer degree and PhD degree in applied science from the University of Liège, Belgium, in 1990 and 1994, respectively. He is currently with the Applied and Computational Electromagnetics (ACE) Unit, Department of Electrical Engineering and Computer Science, University of Liège, as a Senior Research Associate with the FRS FNRS. His research mainly deals with the numerical modeling of coupled problems in electromagnetic systems, including both physical models and numerical techniques coupling. Patrick Dular is the corresponding author and can be contacted at: Patrick.Dular@ulg.ac.be

Ruth V. Sabariego graduated in telecommunication engineering in 1998 at the University of Vigo, Spain. She received the PhD degree in applied sciences from the University of Liège, Belgium, in 2004. From 1998 till 2000, she was a Research Assistant at the Department of Communication Technology, University of Vigo, Spain. She is currently with the ACE Unit, Department of Electrical Engineering and Computer Science, University of Liège, Belgium. Here, she keeps on devoting her research to the domain of applied mathematics in computational electromagnetics.

Laurent Krahenbuhl received the Electrical Engineer degree from the Swiss Federal Institute of Technology (EPFL, Lausanne) and the PhD degree in electrical engineering from the Ecole Centrale de Lyon, France, in 1978 and 1983, respectively. He was by Siemens, Erlangen, Germany, in 1980 1981 and by Cedrat Recherche, France, in 1983 1985. He is currently full researcher with the Centre National de la Recherche Scientifique (CNRS, France), Université de Lyon and Ecole Centrale de Lyon (Ampère). His areas of interest include the numerical computation of electromagnetic fields (using both boundary and finite element methods), the study of special formulations for geometrical singularities (thin layers using modified surface impedances, corners, ...), and homogenization techniques. He is also interested in studies of complex adaptive systems, automatic design and optimization using stochastic methods like genetic algorithms.